Shape resonance for the anisotropic superconducting gaps near a Lifshitz transition: the effect of electron hopping between layers

Supercond. Sci. Technol. **24** (2011) 015012 (10pp) doi:10.1088/0953-2048/24/1/015012

Shape resonance for the anisotropic superconducting gaps near a Lifshitz transition: the effect of electron hopping between layers

Davide Innocenti[1], Sergio Caprara[1], Nicola Poccia[1], Alessandro Ricci[1], Antonio Valletta[1,2] and Antonio Bianconi[1]

[1] Physics Department, Sapienza University of Rome, Piazzale Aldo Moro 2, 00185 Rome, Italy
[2] Institute for Microelectronics and Microsystems, IMM CNR, Via del Fosso del Cavaliere 100, 00133 Roma, Italy

Received 4 August 2010, in final form 15 November 2010
Published 15 December 2010
Online at stacks.iop.org/SUST/24/015012

Abstract
Multigap superconductivity modulated by quantum confinement effects in a superlattice of quantum wells is presented. Our theoretical BCS approach captures the low-energy physics of a shape resonance in the superconducting gaps when the chemical potential is tuned near a Lifshitz transition. We focus on the case of weak Cooper pairing coupling channels and strong pair exchange interaction driven by repulsive Coulomb interaction that allows us to use the BCS theory in the weak-coupling regime neglecting retardation effects, like in quantum condensates of ultracold gases. The calculated matrix element effects in the pairing interaction are shown to yield a complex physics near the particular quantum critical points due to Lifshitz transitions in multigap superconductivity. Strong deviations of the ratio $2\Delta / T_c$ from the standard BCS value as a function of the position of the chemical potential relative to the Lifshitz transition point measured by the Lifshitz parameter are found. The response of the condensate phase to the tuning of the Lifshitz parameter is compared with the response of ultracold gases in the BCS–BEC crossover tuned by an external magnetic field. The results provide the description of the condensates in this regime where matrix element effects play a key role.

(Some figures in this article are in colour only in the electronic version)

1. Introduction

For a long time the conventional theoretical models for high-temperature superconductivity (HTS) in cuprates have been based on a single-component electronic system with a single effective band, while compelling experimental evidence for two bands, resulting from different orbitals, crossing the Fermi level has been reported since 1988 [1]. Unconventional theories for HTS have been proposed focusing on the characteristics of multigap superconductivity [2–4]. The possible role of a Lifshitz transition [5, 6] (also called electronic topological transition (ETT) or quantum phase transition (QPT) of the 2.5th-order) in HTS was discussed in the frame of the single-band model [7]. In 1993 a novel paradigm was proposed that identifies the quantum mechanism for raising the critical temperature in the high-temperature range: the shape resonance in superconducting gaps in multiband systems where the chemical potential is tuned near a Lifshitz transition in one of the bands [8–13].

Over the last 10 years experimental research has been the driving force for shifting the majority of scientists toward the novel paradigm that HTS emerges in complex systems with multiple electronic components in the proximity of a Lifshitz transition. In fact two electronic components at the Fermi level have been found in cuprates by many groups [14–19], showing two (or more) strongly correlated bands with a tendency to phase separation [20, 21]. The two bands in YBaCuO system observed in 1988 [1] are now

confirmed by an increasing number of experiments [22–25] and recent theoretical models consider the new paradigm of a multiband system near a Lifshitz transition [26, 27]. The theory of multiband or multigap superconductivity in the clean limit was developed long ago, but it was accepted only after the discovery of two-gap superconductivity at high temperatures in magnesium diboride MgB_2 [28] and in doped diborides [29–32]. Later, low-temperature multiband superconductivity was found in several materials, such as titanates, ruthenates, borocarbides, and selenides. However, the origin of HTS in MgB_2 has been assigned by many authors to the strong electron–phonon intraband coupling in the σ band. On the contrary, the unique features of multigap superconductivity near a Lifshitz transition [29, 32, 33] have received little attention by the majority of HTS researchers. High-temperature multiband superconductivity was discovered in 2008 in Fe pnictide multilayers. These materials show a clear weak intraband electron–phonon coupling, therefore multigap superconductivity at 50 K in pnictides has determined in the last 2 years the gradual shift of scientific opinion toward the now widely accepted idea that specific features of multigap superconductivity may be essential for the emergence of HTS [34–36]. Recently, the search for HTS has focused on the control of multiband superconductivity in carbon nanotubes [37], graphene bilayers [38], and graphane [39].

Looking for common features of different high-T_c superconducting materials (e.g. cuprates, diborides, and pnictides), one could list the following: first, multigap superconductivity; [40] second, multiple electronic components; [41] third, a heterostructure at the atomic limit, made of superconducting atomic layers intercalated by spacers made of a different material, forming a superlattice [8, 9] as shown in figure 1; fourth, the tuning of the Fermi energy (using any physical, chemical or material manipulation method, such as doping and superlattice misfit strain) in order to reach a particular point in the electronic band structure [42–45]. These are the features which were proposed to be essential for the synthesis of new high-T_c superconductors, with T_c eventually reaching room temperature, in [8–10]. The particular condition yielding high T_c was thereby identified as the tuning of the Fermi energy at a *shape resonance* for the superconducting gaps near a Lifshitz transition. In this work we first discuss the fundamental points of shape resonances in multiband superconductors made of a first two-dimensional (2D) cylindrical Fermi surface and a second Fermi surface, tuning the chemical potential near the Lifshitz transition. We present the results for the system of weak intraband coupling so the system is well described by the BCS weak-coupling limit, and we consider a case where the interband pairing is the dominant interaction so that it could describe the case of pnictides where the interband pairing is the dominant interaction. In this regime we investigate the effect of variable electron hopping between the layers that is the characteristic feature of superlattices of superconducting layers at the atomic limit.

2. Shape resonances for superconducting gaps

The concept of *shape resonance* for superconducting gap parameters was first introduced by Blatt and Thompson for a single 2D membrane [46] and it has been developed for a single nanowire [47]. The *shape resonance* for the superconducting gaps in superlattices of quantum wells (quantum layers, quantum wires, and quantum dots) [8, 9, 11] has been proposed to yield three-dimensional (3D) superconductors. Shape resonances in a superlattice of stripes in cuprates [48–50], and pnictides [36], of layers in diborides [33, 51–54], and in a superlattice of nanowires in carbon nanotubes, have been discussed [37]. The novel scenario for a multiband system with a dominant role for interband pairing and negligible intraband coupling was proposed before the discovery of pnictides.

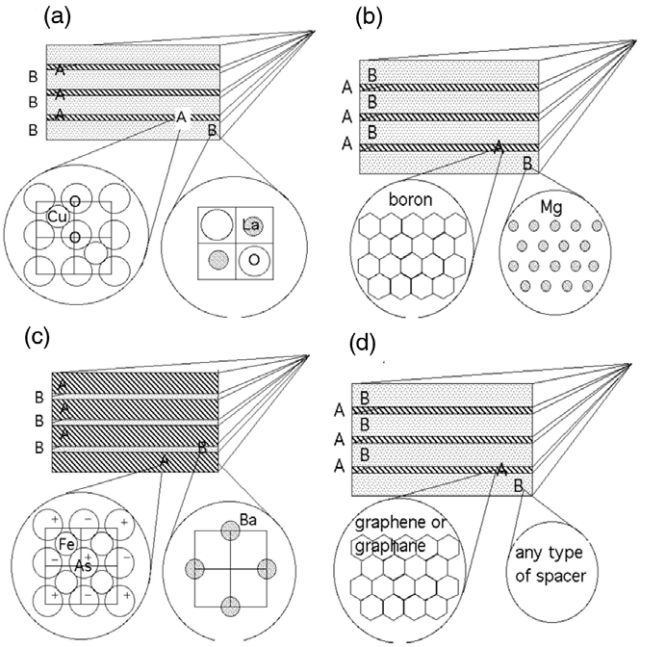

Figure 1. Pictorial view of artificial heterostructures realized as superlattices of stacked planes, with particulars of the superconducting layer and of the spacer layers, in four different families of compounds: (a) cuprates, (b) magnesium diborides, (c) iron pnictides, and (d) graphene or graphane layers.

The definition of *shape resonance* in the theory of superconductivity [46] is borrowed from nuclear physics. In 1929–1930 Ettore Majorana first developed a theoretical model to describe the artificial disintegration of nuclei by bombardment with α-particles [55–57]. By following the quantum dynamics of a state resulting from the superposition of a discrete state with a continuum one, whose interaction is described by a given potential term, Majorana first applied the concept of quasi-stationary states interacting with the continuum [55–57]. The theory of a shape-elastic scattering cross section for nucleon–nucleus resonances, where the total energy of incoming or outgoing particles and the quasi-stationary states of the compound nucleus are nearly degenerate, was developed in the 1950s by Blatt, Feshbach and de Shalit [58–60]. The *shape resonance* in nuclear scattering from a potential exhibits characteristic peaks, as a function of energy, for values of energy such that an integral number of wavelengths fits within the nuclear potential well. Shape resonances have been measured in electron–atom scattering [61] and electron–molecule scattering [62, 63]

experiments. The name *Feshbach resonance* was coined to indicate a particular shape resonance, where the quasi-bound state is near zero energy [63]. The Feshbach resonance in atomic association and dissociation processes occurs in ultra-dilute and ultracold atomic gases where the energy of a diatomic molecule (tuned by an external magnetic field) is degenerate with the chemical potential of the atomic gas [64]. In this condition the exchange interaction gives the Feshbach resonance. The discovery that in boson and fermion ultracold gases the energy of the diatomic molecule can be tuned (by means of a magnetic field) above and below the continuum threshold has led to the realization of Bose–Einstein condensation (BEC) in boson gases and of the BCS–BEC crossover in fermion gases driven by the Feshbach resonance [65–67]. Therefore the shape resonance and Feshbach resonance belong to the class of Majorana–Fano–Feshbach resonances due to configuration interaction effects between open and closed scattering channels described by the Feshbach–Fano partitioning method [68–70]. In a multiband superconducting system, when the chemical potential is tuned at the Lifshitz transition in one of the bands, the pairs of electrons at the Lifshitz transitions are in a quantum critical point where the group velocity of electrons goes to zero and they form bosonic pairs that can be considered the equivalent of the Majorana quasi-stationary states or the diatomic molecule in the magnetic field in ultracold gases.

In superlattices, the shape resonance [11–13, 37, 53] in the superconducting gaps appears when the Fermi energy of electrons in a band is tuned around the Lifshitz transitions [11] in a different band. There are several types of Lifshitz transitions:

> Type (I) when the Fermi energy crosses the band edge, at $E_{\rm edge}$, with the appearance or disappearance of a new Fermi surface (FS).
> Type (II) when the Fermi energy crosses the electronic topological transition $\mathrm{ETT}_{\rm 3D-2D}$ where one FS changes from 3D to 2D (i.e. from 'spherical' to 'cylindrical') or vice versa, with the opening or closing of a neck in a tubular FS.
> Type (III) at the singular point where the FS changes from 2D to one-dimensional (1D) or vice versa, with the change of FS topology from a closed FS circle to disconnected Fermi arcs [50]. Once the heterostructure of materials selected as the building blocks for the superconducting units and for the spacer layers has been synthesized with its structural parameters, the tuning of the Fermi level at an ETT can be controlled by means of: (i) the 'charge transfer' between the superconducting layers and the 'spacers'; (ii) the superlattice misfit strain [71–73] between the superconducting and spacer layers; (iii) the thickness of the spacers; (iv) the ordering of dopants in the spacer; (v) the superstructures in the superconducting layers forming stripes; (vi) pressure.

3. Breakdown of the standard BCS approximations

The heterostructures at the atomic limit of superconducting units, where the chemical potential is tuned at a type I Lifshitz transition (appearance or disappearance of a new FS spot) and the type II Lifshitz transition (opening a neck in a FS), where the superconducting gaps show a shape resonance, have been called *superstripes* [74–76]. From the theoretical point of view, the shape resonance implies the breakdown of two main approximations of the standard BCS theory of superconductivity: (1) the infinite distance of the Fermi energy from the band edges, which is reasonable whenever the energy cut-off for the pairing interaction, ω_0, is much smaller than the Fermi energy $E_{\rm F}$ (as measured from the nearest singular point in the electron spectrum): in this case the electron density of states (DOS) can be taken as nearly constant within an energy window of the order of ω_0; (2) the single-band approximation, which is altogether reasonable in the dirty limit, when impurity scattering mixes the various electron components yielding an effective single-band system.

The situation in which the first approximation breaks down (e.g. when the Fermi energy falls near an electronic topological transition) has been called the van Hove scenario [77–81], or the Pomeranchuk instability scenario [82–84], belonging to the class of quantum phase transition scenarios investigated for pairing in single-band superconductivity [85–88]. While these scenarios have been proposed for cuprates assuming a single-band approximation, recently there has been increasing evidence for the occurrence of multiband superconductivity in cuprates as well [1, 14–20, 22–28, 41, 89, 90].

As far as the second approximation is concerned, as we have recalled above, the very concept of multiband superconductivity is meaningful only in the clean limit. Indeed, in nearly all metals and alloys several bands cross the Fermi level, but impurity scattering leads to a mixing of the electron states. Therefore, the single-band description, which is adopted, e.g. in the standard BCS theory, is a reasonable approximation in the dirty limit. However, several experiments in doped diborides have shown that the clean limit is robust in heterostructures at the atomic limit where both the different parity of the bands and their different spatial location forbid the mixing of the different electron states at the Fermi surfaces [11]. Nowadays it is commonly accepted that the dirty-limit approximation breaks down in magnesium diboride, in pnictides, in superlattices of carbon nanotubes, in graphene and graphane layers, and multigap superconductivity may also emerge in the presence of lattice disorder due to dopants and misfit strain of the superlattice, when these are not apt to mix the different electronic components.

Another crucial feature of multiband superconductivity is that, beyond the standard intraband attractive interactions that promote pairing within each band, exchange-like interband interactions, that scatter Coopers pairs from one band to another, become relevant. In the hypothetical absence of interband interactions, each band would be characterized by its own superconducting critical temperature. Arbitrarily weak interband interactions lead to a single critical temperature, as in the proximity effect. It is important to notice that interband interactions are generically repulsive, and in this case interband pairing leads to condensate wavefunction with opposite signs (the so-called $s\pm$ pairing) [2–4, 11, 34]. In the shape resonance

scenario for multiband superconductivity, the control of the ratio between the intensity of exchange-like interband pairing and intraband Cooper pairing, by material design techniques, is crucial.

4. Two band superconductivity at a band edge

In this work we study the shape resonance in the case when the Fermi energy is tuned at a band edge energy $E_{\rm edge}$ in one of the bands in a multiband superconductor. In particular we focus on superlattices of metallic layers, with finite hopping probability between the metallic layers. The universal feature of band edges in a superlattice of metallic layers is that the small FS appearing or disappearing as the Fermi energy crosses the band edge has a 3D topology, due to finite electron hopping between the layers separated by a finite potential barrier. We consider the interesting case where the electron hopping between layers is so small that the transverse band dispersion ξ due to hopping between layers is much smaller than the energy separation between the subbands. In these superlattices the FS appearing or disappearing as the Fermi energy crosses the band edge has a 3D topology in the range $0 < E_{\rm F} - E_{\rm edge} < \xi$. When the Fermi energy crosses the van Hove singularity, an $\rm ETT_{3D-2D}$ of the Lifshitz type called 'opening a neck' takes place, with the FS changing topology from closed to tubular at $E_{\rm F} - E_{\rm edge} = \xi$.

It has been shown [11, 36] that the optimum amplification of the critical temperature occurs when ξ is of the order of the energy cut-off of the interaction, ω_0. In this case, in the narrow energy range $3\omega_0$ where the chemical potential crosses both the band edge and the $\rm ETT_{3D-2D}$, the condensate in the newly appearing FS undergoes a crossover from a mixed Bose–Fermi regime to the Fermi BCS regime. For example, in the regime $-1 < (E_{\rm F} - E_{\rm edge})/\omega_0 < 0$, the electron states associated with the newly appearing FS are unoccupied in the normal state, and a BEC-like condensate of pairs with bosonic character is formed below the critical temperature. In the range $0 < (E_{\rm F} - E_{\rm edge})/\omega_0 < 1$, all the few normal state electrons in the newly appearing 3D FS condense below $T_{\rm c}$, with the breakdown of the standard approximation $(E_{\rm F} - E_{\rm edge})/\omega_0 \gg 1$. In the range $0 < (E_{\rm F} - E_{\rm edge})/\omega_0 < 1$, in the case under discussion, $\xi = \omega_0$, the new FS has a 3D topology. The $\rm ETT_{3D-2D}$ plays a key role in the configuration interaction between pairing channels in different bands in the range $0 < (E_{\rm F} - E_{\rm edge})/\omega_0 < 2$.

We are interested in the evolution of superconducting gaps in the two bands and of the critical temperature in the narrow energy range where the Feshbach-like shape resonance takes place in superconducting gaps. So, we consider a first large 2D FS in the standard BCS approximation (i.e. where the standard BCS approximation is valid, large $E_{\rm F}/\omega_0$ ratio, with $E_{\rm F}$ far from band edges) that coexists with the appearance of a second small FS, where the standard approximation breaks down (small $E_{\rm F}/\omega_0$ ratio, with $E_{\rm F}$ close to both the band edge and $\rm ETT_{3D-2D}$) (see figure 2).

This simple model is apt to capture the physics emerging from experiments in doped diborides [33], cuprates [26, 27], and pnictides [91–97]. Moreover it represents the optimal case to obtain the enhancement of critical temperature via the shape resonance mechanism [11]. It describes the multiband pairing at the bottom or top of 2D bands in a generic superlattice of layers. Here, the effective potential barrier and the thickness of the spacer layers are selected to adjust the electron hopping between superconducting layers and the transverse energy dispersion ξ of the order of the energy cut-off ω_0 of the interaction.

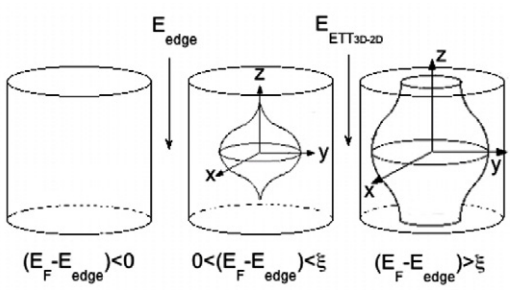

Figure 2. Pictorial view of the evolution of the FS of the two-band electronic system near a band edge crossing two Lifshitz transitions. The chemical potential is tuned so that $E_{\rm F}$ crosses the band edge $E_{\rm edge}$ of the second band (the type I Lifshitz transition) and the 3D–2D ETT at $E_{\rm 3D-2D}$ (the type II Lifshitz transition). Here, ξ is the transverse band dispersion. On the left side a first large 2D FS coexists with a second tubular 2D FS; with decreasing $E_{\rm F}$ and crossing the energy $E_{\rm 3D-2D}$ where the second FS undergoes a 3D–2D ETT changing its topology, the tubular 2D FS becomes a closed 3D FS, as shown in the central panel; only the first large 2D FS remains when the chemical potential is moved below the band edge energy $E_{\rm edge}$ of the second band as shown in the left panel.

The shape resonance is determined by the relative strength of the intraband coupling constants and the interband coupling constant, determined by the type of material forming the superconducting layers and the type of material forming the spacers. We consider here the case, typical of pnictides, where the intraband attractive coupling strength is weak in both the first and second subbands. We have obtained the evolution of the superconducting gaps from below the edge, in the mixed Fermi–Bose regime, to above the ETT in the Fermi-like regime. Direct evidence for the quantum interference effect between pairing channels is provided by minima in the gap parameter for electrons in the large FS. We report the evolution of this scenario with increasing exchange interband pairing. We also investigate the effect of the variation of the transverse dispersion ξ that can be changed by changing the separation space between layers. These results can explain the differences among 1111 pnictides with changing the rare earth ionic radius, and the difference between 1111 and 122 pnictides where the spacer layers change in the superlattice while the superconducting layers are kept fixed.

Finally, we show that the plots of the BCS gap ratios versus the critical temperature display significant changes in the different superconducting regimes of the Feshbach-like shape resonance. These plots can be easily compared with experimental data and provide a very good experimental test for the theory of the Feshbach-like shape resonance.

There is a clear analogy between the Bose–Fermi crossover case studied here and the BEC–BCS crossover in ultracold Fermi gases [98]. The theory presented here follows

Blatt's approach [46], and is appropriate for dealing with the case of a chemical potential near a band edge since the equation for the gaps is solved together with the equation for the chemical potential in the superfluid phase. In fact, like for the BCS–BEC crossover and as shown by Leggett [99], the BCS wavefunction corresponding to an ensemble of overlapping Cooper pairs at weak coupling considering a contact interaction (BCS regime) evolves to non-overlapping pairs with bosonic character as the density decreases at the band edge (BEC regime). The BCS theory remains valid in this limit if the BCS equation for the gap is coupled to the equation that fixes the fermion density so that the chemical potential μ becomes strongly renormalized below the critical temperature with respect to the Fermi energy $E_{\rm F}$ of the non-interacting system.

In ultracold gases the energy of the bound state of the diatomic molecule above or below the continuum is tuned by a magnetic field. In the present case of superlattices the chemical potential can be tuned near the ETT of a narrow band, for example by superlative misfit strain.

5. The two band model in a superlattice of metallic layers

As pointed out above, the standard multiband BCS theory in the weak-coupling limit (or the Eliashberg theory in the strong-coupling limit) [2–4] assumes a DOS which is (at least approximately) constant within a window of thickness $2\omega_0$ around the Fermi energy. This assumption is certainly not valid if the chemical potential is located near a band edge or close to a van Hove singularity of a superlattice of metallic layers.

Near the band edges in the ℓth band, where $\nabla_{\mathbf{k}} E_\ell = 0$, the energy of an electron can be approximated by a free electron dispersion law $E_{\ell,\mathbf{k}} = E_\ell + (\mathbf{k}^2/2m_\ell)$, where m_ℓ is the electron effective mass at the band edge. Therefore, one can use the free electron approximation in a narrow region around the band edge in the case when the band width is much larger than $2\omega_0$, the energy range of interest for pairing. In the case of interest here, however, while this approximation is valid in the x, y plane of the superconducting layers, it is certainly not valid in the z direction, where the dispersion is of the order of ω_0. In this case, an anisotropic band with weak dispersion in the z direction and larger dispersion in the x, y plane above the band edge of the second band should be adopted:

$$E^{\rm 3D}_{2,\mathbf{k}} = E_2 + E(k_z) + \frac{k_x^2 + k_y^2}{2m_\parallel} \qquad (1)$$

where $E(k_z)$ is the actual energy dispersion in the periodic potential of the superlattice and $m_\parallel$ is the effective mass in the x, y plane. This situation is obtained within a model where a free electron gas is confined in a potential which is periodic in the z direction:

$$\mathcal{W}(z) = \sum_{n=-\infty}^{n=+\infty} \mathcal{W}_{\rm b}(z - nd), \qquad (2)$$

where $\mathcal{W}_{\rm b}(z) = -V_{\rm b}$ for $|z| \leqslant L/2$ and $\mathcal{W}_{\rm b}(z) = 0$ for $L/2 < |z| < d/2$, L is the width of the confining well

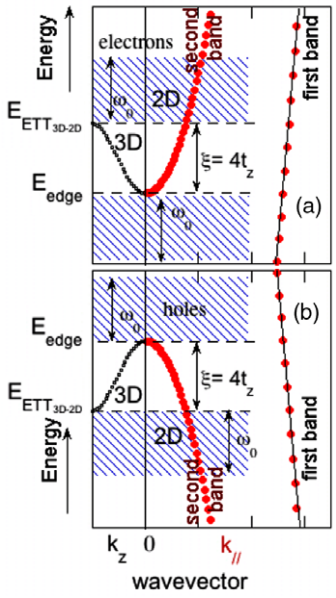

Figure 3. The shape resonance occurs by tuning the Fermi energy near the band edge $E_{\rm edge}$ of a second electron-like band (upper panel) or a second hole-like band (lower panel). The second band coexists with a large first band (with the Fermi energy far from its edges) that has a free electron like dispersion. The second band has a free electron dispersion in the direction of the electron wavevector parallel to the plane ($k_\parallel$) while in the perpendicular direction (k_z) of the superconducting layers it is determined by a periodic potential barrier determined by the superlattice. This second band has a 3D character in the energy range between the band edge and the van Hove singularity energy $E_{\rm ETT_{3D-2D}}$. The band dispersion is $\xi = 4t_z$, where t_z is the electron hopping integral between the layers.

and d is the periodicity of the superlattice in the z direction. This periodic potential mimics the phenomenology, e.g. of the pnictides, diborides, and stacks of graphene layers made of a superlattice of stacked planes, as shown in figure 1. The confining potential generates a band structure organized in subbands. Each subband has a dispersion in the transverse direction, as shown in figure 2, that gives a Fermi surface with 3D topology, with a closed isoenergetic surface, near the lower band edge $E_{\rm edge} = E_{\ell,L}$, and a 2D character, with isoenergetic surfaces open in the z direction, above some energy threshold $E_{\rm ETT_{3D-2D}} = E_{\ell,T}$. The present model is apt to describe quantum interference phenomena between different scattering channels in a large and a small FS which are the object of this work, when the chemical potential μ of the system is tuned near the bottom of the ℓth subband, within a window of width $4\omega_0$. In the energy window of width $2\omega_0$ the first band, with a large 2D tubular FS, has a constant DOS N_1. The second FS appears as the Fermi energy crosses the level $E_{\rm edge} = E_{\ell,L}$, and changes from closed 3D to tubular 2D topology as the Fermi energy crosses the level $E_{\rm ETT_{3D-2D}} = E_{\ell,T}$, as shown in figure 2. The model for an electron-like FS can be easily extended to a hole-like FS as shown in figure 3. The DOS of the second FS N_2 near the edge has the typical 3D behavior.

In order to solve the BCS equations in the shape resonance scenario it is necessary to determine the electron wavefunction. Using the model of a free electron gas confined

in a superlattice, the wavefunction of electronic states can be obtained by solving the Schrödinger equation, so that we can calculate the anisotropic **k**-dependent gaps in the wavevector space and the interference between the intraband pairing channels and the pair exchange determined by the interband pairing terms. The solution of the Schrödinger equation for the 1D periodic potential of the superlattice of layers allows us to also calculate the gaps in correspondence of the 3D to 2D electronic transition ETT_{3D-2D} at the van Hove singularity, beyond the standard BCS approximations [46, 50].

Going from a single slab [46] to a 3D superlattice [50], a 3D condensate is formed, reducing the effect of fluctuations of the superconducting order parameter, which suppress the mean-field superconducting T_c. The crossover from 2D to 3D can be described in our model by changing from an infinite potential barrier between the planes of the superlattice in the z direction, provided by spacer layers, to a finite barrier (V_b). This yields a finite hopping term that broadens the sharp discontinuity of the DOS of a pure 2D band. This broadening increases the width of the shape resonance and, at the same time, yields a 3D condensate. Moreover, it is possible to design artificial superlattice heterostructures at the optimum shape resonance condition, i.e. where the value of the potential barrier V_b and its width are such that the subband dispersion in the z direction, ξ, is of the order of the energy cut-off, ω_0, of the interaction. Therefore, it is possible to tune the system to the optimum shape resonance condition, achieving an enhancement of the critical temperature.

The intrinsic **k**-dependence of the pairing interaction $\mathcal{V}^{\ell,\ell'}_{\mathbf{k},\mathbf{k}'}$ in the superlattice with wavevector $\mathbf{k}_z$ induces a structure in the **k**-dependent interband coupling interaction for the electrons that determines the quantum interference between the electron pair wavefunction in different subbands of the superlattice [11]. We calculate the term $\mathcal{V}^{\ell,\ell'}_{\mathbf{k},\mathbf{k}'}$ following our previous work on a superlattice of wires [50], determining the matrix elements of local interaction potential and then introducing a cut-off with two θ functions

$$\mathcal{V}^{\ell,\ell'}_{\mathbf{k},\mathbf{k}'} = \tilde{\mathcal{V}}^{\ell,\ell'}_{\mathbf{k},\mathbf{k}'}\theta(\omega_0 - |\xi_{\ell,\mathbf{k}}|)\theta(\omega_0 - |\xi_{\ell',\mathbf{k}'}|) \tag{3}$$

where $\mathbf{k} = \mathbf{k}_z$ ($\mathbf{k}' = \mathbf{k}'_z$) is the superlattice wavevector in the z direction, perpendicular to the planes, of the initial (final) state in the pairing process, and

$$\tilde{\mathcal{V}}^{\ell,\ell'}_{\mathbf{k},\mathbf{k}'} = \frac{c_{\ell,\ell'}}{N_0(E_F)V_{3D}} I^{\ell,\ell'}_{\mathbf{k},\mathbf{k}'}, \tag{4}$$

where $N_0(E_F)$ is the DOS at E_F for a free electron 3D system, V_{3D} is the volume of the system

$$I^{\ell,\ell'}_{\mathbf{k},\mathbf{k}'} = -d\int_d \psi_{\ell,-\mathbf{k}}(z)\psi_{\ell',-\mathbf{k}'}(z)\psi_{\ell,\mathbf{k}}(z)\psi_{\ell',\mathbf{k}'}(z)\,\mathrm{d}z \tag{5}$$

and $\psi_{\ell,\mathbf{k}}(z)$ are the eigenfunctions in the superlattice of quantum wells, normalized so that $\int_d \mathrm{d}z\,|\psi_{\ell,\mathbf{k}}(z)|^2 = 1$. The use of a single cut-off in two-band superconductivity has been justified in detail in [100].

The dimensionless factor $c_{\ell,\ell'} = (-1)^{\delta_{\ell,\ell'}} c^0_{\ell,\ell'}$ assumes positive values for $\ell = \ell'$ (intraband Cooper pairing) and negative values for $\ell \neq \ell'$ (repulsive exchange-like interband pairing, with $c_{\ell,\ell'} = c_{\ell',\ell}$) and measures the relative intensity of intraband and interband pairing strength. In fact, it multiplies the **k**-dependent integral and therefore permits us to simulate the behavior of different superconductive multilayer compounds controlling the ratio between intensities of intraband and interband pairings.

In order to determine the gaps and chemical potential self-consistently and to calculate the superconductive T_c we use iterative solving methods for the coupled BCS-like equations

$$\Delta_{\ell,\mathbf{k}}(\mu) = -\frac{1}{M}\sum_{\ell',\mathbf{k}'}\frac{\mathcal{V}^{\ell,\ell'}_{\mathbf{k},\mathbf{k}'}\Delta_{\ell',\mathbf{k}'}}{2\sqrt{(E_{\ell',\mathbf{k}'}-\mu)^2+\Delta^2_{\ell',\mathbf{k}'}}}, \tag{6}$$

$$\rho = \frac{1}{d^2}\sum_{\ell,\mathbf{k}}\left[1 - \frac{E_{\ell,\mathbf{k}}-\mu}{\sqrt{(E_{\ell,\mathbf{k}}-\mu)^2+\Delta^2_{\ell,\mathbf{k}}}}\right], \tag{7}$$

starting with an initial gap parameter equal to a constant and an initial chemical potential equal to the Fermi level in the normal state and assuming the convergence occurred for relative variation of the gap and charge density ρ less than 10^{-6}. Here M is the total number of wavevectors $\mathbf{k}'$ and ρ is the electron density. The superconducting critical temperature T_c is calculated by iteratively solving the linearized equation

$$\Delta_{\ell,\mathbf{k}} = -\frac{1}{2M}\sum_{\ell',\mathbf{k}'}\mathcal{V}^{\ell,\ell'}_{\mathbf{k},\mathbf{k}'}\frac{\tanh\left(\frac{E_{\ell',\mathbf{k}'}-\mu}{2T_c}\right)}{E_{\ell',\mathbf{k}'}-\mu}\Delta_{\ell',\mathbf{k}'}, \tag{8}$$

until the vanishing solution is reached with increasing temperature. Here, the gaps depend on the superlattice wavevector **k** as well as on the subband index. Hence, T_c and the gap at a given point of **k**-space become implicit functions of all the different values of the gaps in the entire **k**-space.

In the standard BCS theory, where the Fermi energy is far from the band edges, the relative variation of the chemical potential going from the normal to the superconducting state is expected to be negligible. This is not true when the chemical potential is tuned near the band edge of the second band. In fact, our calculation yields a significant variation of the chemical potential in the superconducting phase, as a function of the charge density. A relative variation of the chemical potential going from the normal to the superconducting phase, as large as 10^{-3}, is obtained near the band edge and at ETT_{3D-2D}, within a range $4\omega_0$. The variation starts to be large, as compared with the standard BCS result, in proximity of the Bose–Fermi crossover regime below the band edge up to well beyond ETT_{3D-2D}.

The Feshbach-like shape resonance regime occurs properly in correspondence to this large variation of the chemical potential between the normal and superconducting phases. Our theoretical approach provides a direct measure of the gap, at a given point of **k**-space anisotropy for both intraband and exchange interband terms. The intraband distributions of the two bands show different shapes and widths and have a different range of values. The resulting matrix of coupling terms is obtained exclusively from the eigenfunctions of the superlattice and is asymmetric.

Below, we present numerical results for the solution of the self-consistency equations which determines the values of the gap in the large FS and in the small FS. We discuss the behavior of Δ_1 and Δ_2, defined as average values of the gaps on the corresponding branches of the Fermi surface, and of the critical temperature T_c.

We discuss the case where the coupling term in the second band is smaller than in the first band (called here the pnictide-like case). This case emphasizes the role of the exchange-like interband pairing and uses the BCS weak limit for interactions for contact interactions, neglecting retardation effects. In the extreme case when the intraband coupling in the second band is zero, the pairs in the second band are only formed thanks to interband exchange-like pairing.

Therefore in this approach we consider the intraband coupling $c_{1,1}$ for the band that does not show the Lifshitz transition, the intraband coupling $c_{2,2}$ for the one that shows the Lifshitz transition and the interband coupling $c_{1,2}$ for the exchange-like pairing.

Figure 4 shows the case of weak coupling in the second band where the intraband coupling parameter ratio is fixed at $c_{2,2}/c_{1,1} = 0.45$. The critical temperature T_c (panels (a)), the ratio $2\Delta_1/T_c$ (panel (b)), and the ratio $-2\Delta_2/T_c$ (panel (c)) are plotted as functions of the reduced Lifshitz parameter $(\mu - E_{2,L})/\omega_0$. The different curves in each panel represent the cases of different interband pairing strengths ($c_{1,2}/c_{1,1} = -0.68, -0.91, -1.04, -1.59, -2.73$). In correspondence of the largest interband pairing strength examined here, $c_{1,2} = -2.73$, we have obtained critical temperatures as large as 50 K, in the range $1 < (\mu - E_{2,L})/\omega_0 < 2$. The antiresonance in the first gap appears when the ratio $2\Delta_1/T_c$ reaches the minimum value, which can be much smaller than the standard BCS value ($2\Delta/T_c = 3.53$). The antiresonance appears in the range $-1 < (\mu - E_{2,L})/\omega_0 < 0$ and moves from -1 to zero, decreasing the interband pairing. Moreover the second superconducting gap values turn out to be nonzero even before the lower band edge $E_{2,L}$ is reached. We notice that the maximum T_c is reached in the BCS regime zone near the type II Lifshitz transition (ETT_{3D-2D}).

Iron pnictide superconductors are certainly more three-dimensional than cuprates (they have a quasi-2D electronic structure), but the dimensionality of electronic structure in these compounds is also less clear, in fact even if some band structure works predict strong k_z dispersion [101], other works predict weak dispersions in AFe_2As_2 and ReOFeAs [102], determined mainly by the Fe d-orbitals of FeAs layers. Furthermore, many angle-resolved photoemission spectroscopy experiments [103–108] reveal weak k_z dependences for the bands' electronic structure; in fact most of the band dispersion of 1111 and 11 iron pnictides, like LaOFeAs and NaFeAs [109, 110], are in the range of 20–40 meV. In 122 undoped pnictides, like $BaFe_2As_2$, the k_z dispersion is rather small [111], although in $BaFe_{2-x}Co_xAs_2$, with increasing Co concentration, the k_z dispersion increases up to 120 meV [112].

Figure 5 shows the effect of the variation of out-of-plane dispersion on the shape resonance, in the case of weak coupling in the second band (the so-called iron pnictide case) for strong interband pairing. The DOS of the second subband for different

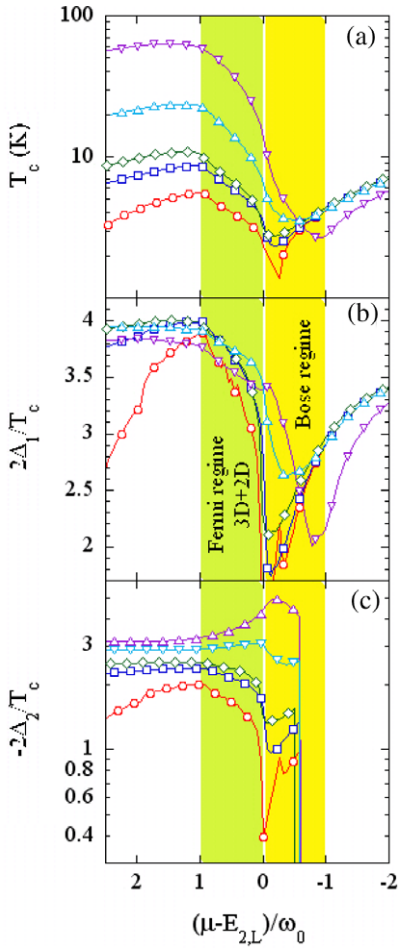

Figure 4. The case of weak coupling in the second band (the so-called pnictide case) where the intraband coupling parameters ratio is fixed at $c_{2,2}/c_{1,1} = 0.45$. The critical temperature T_c (panel (a)), the ratio $2\Delta_1/T_c$ (panel (b)) and the ratio $-2\Delta_2/T_c$ (panel (c)) are plotted as functions of the reduced Lifshitz parameter $(\mu - E_{2,L})/\omega_0$. The different curves in each panel represent the cases of different interband pairing strengths: the case for $c_{12}/c_{11} = -2.73$ (open upward pointing triangles); the case for $c_{12}/c_{11} = -1.59$ (open downward pointing triangles); the case for $c_{12}/c_{11} = -1.04$ (open diamonds); the case for $c_{12}/c_{11} = -0.91$ (open squares) and shows the case for $c_{12}/c_{11} = -0.68$ (red curve with open circles). For the largest case of interband pairing strength $c_{1,2}$ considered here, the critical temperature reaches 300 K in the range $1 < (\mu - E_{2,L})/\omega_0 < 2$. The shape resonance antiresonance appears as a minimum in the critical temperature for $(\mu - E_{2,L})/\omega_0 = -1$ for the higher interband repulsive interaction and moves towards $(\mu - E_{2,L})/\omega_0 = 0$ for the smaller interband repulsive interaction. The ratio $2\Delta_1/T_c$ for the first band shows maxima and minima like the critical temperature. On the contrary the ratio $2\Delta_2/T_c$ shows a minimum at $(\mu - E_{2,L})/\omega_0 = 0$ and it has a maximum at the value of maximum T_c for weak interband repulsive coupling; on the contrary it exhibits a maximum in the Bose-like regime (yellow region) $(0 > \mu - E_{2,L})/\omega_0 > -1$ and a minimum value in correspondence of the maximum T_c for very strong interband repulsive pairing.

dispersions ($\xi = 110$, 68 and 36 meV), as a function of the reduced Lifshitz parameter $(\mu - E_{2,L})/\omega_0$, is shown as an inset in panel (a). The intraband and interband coupling parameter ratios ($c_{2,2}/c_{1,1} = 0.45$ and $c_{1,2}/c_{1,1} = -3.6$, with $c_{1,1} = 0.22$) are fixed. The critical temperature, panel (b), the

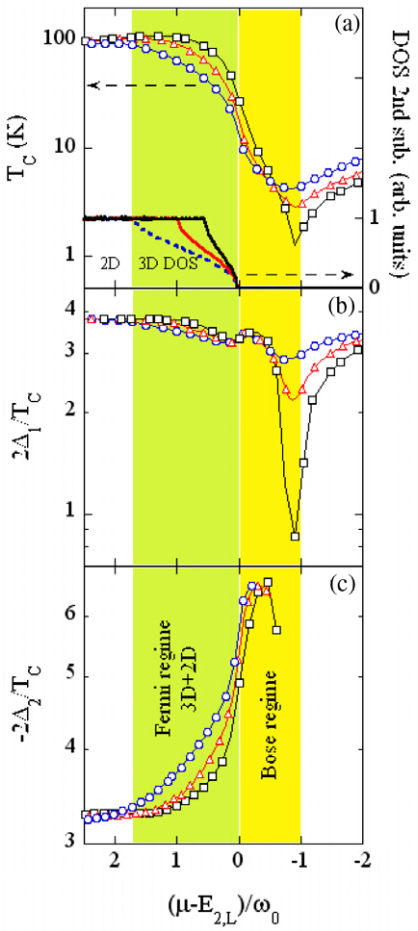

Figure 5. The effect of the variation of transverse dispersion on the shape resonance, the case of weak coupling in the second band (the so-called iron pnictide case) for strong interband repulsive interaction. The intraband and interband coupling parameter ratios ($c_{2,2}/c_{1,1} = 0.45$ and $c_{1,2}/c_{1,1} = -3.6$, with $c_{1,1} = 0.22$) are fixed. The critical temperature (panel (a)), the ratios $2\Delta_1/T_c$ (panel (b)) and $-2\Delta_2/T_c$ (panel (c)) as a function of the reduced Lifshitz parameter $(\mu - E_{2,L})/\omega_0$ are plotted for $\xi = 110$ (blue curve with open circles), 68 (red curve with open triangles) and 36 meV (black curve with open squares). This last case is close to the case of a single quantum well. We also plot the DOS of the second subband in the inset of panel (a). The ratio $2\Delta_1/T_c$, probing the pairing channel in the first large FS, exhibits two minima due to the negative interference effect (or antiresonance) typical of shape resonances, at the band edge $(\mu - E_{2,L})/\omega_0 = 0$ and the ETT $(\mu - E_{2,L})/\omega_0 = -1$. The antiresonance effect in the large FS increases for decreasing dispersion in the second band. The value of the second superconducting gap is nonzero even before the lower band edge $E_{2,L}$ is reached. In the second band the maximum value of the ratio is always reached in the Bose regime and remains the same, $-2\Delta_2/T_c \simeq 6.7$, for all dispersion values.

ratios $2\Delta_1/T_c$, panel (c), and $-2\Delta_2/T_c$, panel (d), are plotted as a function of the reduced Lifshitz parameter $(\mu - E_{2,L})/\omega_0$. The minima of the ratio $2\Delta_1/T_c$, probing the pairing channel in the first large Fermi surface show two minima due to the negative interference effect or antiresonance typical of shape resonances at the band edge $(\mu - E_{2,L})/\omega_0 = 0$ and the ETT $(\mu - E_{2,L})/\omega_0 = -1$. The antiresonance effect in the large FS increases for decreasing dispersion in the second band.

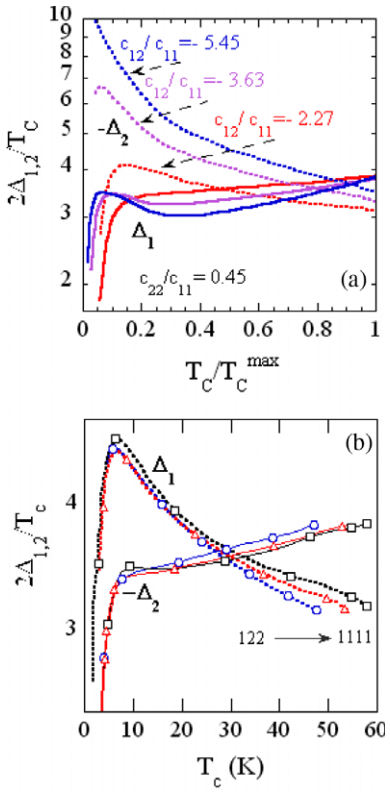

Figure 6. (a) The ratios $2\Delta_1/T_c$ and $-2\Delta_2/T_c$ as function of the ratio T_c/T_c^{max}, in the case of weak coupling in the second band, with fixed $c_{2,2}/c_{1,1} = 0.45$, $c_{1,1} = 0.22$ and interlayer dispersion $(\xi/\omega_0 = 1)$, for three cases of different interband coupling parameters ($c_{1,2}/c_{1,1} = -2.27$, -3.63, and -5.45) ratio. (b) The ratios $2\Delta_1/T_c$ and $-2\Delta_2/T_c$ as functions of T_c in the case of weak coupling in the second band with fixed $c_{2,2}/c_{1,1} = 0.45$, $c_{1,1} = 0.22$ and interlayer dispersion $(\xi/\omega_0 = 1)$, and in the case of weak coupling in the second band with fixed $c_{1,2}/c_{1,1} = 0.45$, $c_{1,1} = 0.22$ and interlayer dispersion $\xi = 110$ (blue curve with open circles), 68 (red curve with open triangles) and 36 meV (black curve with open squares).

The value of the second superconducting gap is nonzero even before the lower band edge $E_{2,L}$ is reached. In the second band, the maximum value of the ratio is always reached in the Bose regime and remains the same, $-2\Delta_2/T_c \simeq 6.7$, for all dispersion values.

Using STM spectroscopy it is now possible to measure the gaps and the critical temperature in the same set of experiments. Therefore the BCS gap ratios $2\Delta_1/T_c$ and $-2\Delta_2/T_c$ as functions of the ratio T_c/T_c^{max} can be measured directly for different samples of different gate voltages tuning the chemical potential. The present theory is able to predict these curves, and we show that these curves provide a direct measure of the relevance of interband coupling versus Cooper pairing. In figure 6 we show the case for strong interband repulsive interaction and weak coupling for Cooper pairing. We keep the ratio $c_{2,2}/c_{1,1} = 0.45$, $c_{1,1} = 0.22$ and $\xi/\omega_0 = 1$ constant and we present the expected behavior of these curves for strong interband interaction. The BCS gap ratio parameters are plotted for three cases of different interband coupling parameters. When the interband repulsive term is dominant, the BCS gap ratio is the same in both bands at

the maximum critical temperature. The difference between the gap ratios diverges, decreasing the critical temperature. This behavior is very similar to case of cuprates in fact in the underdoped region where the critical temperature goes to zero and while a first BCS-like gap decreases with decreasing critical temperature, the second gap (called the pseudogap) increases with decreasing critical temperature.

We have investigated the effect of band dispersion for a case of moderate relevance of the interband pairing such that there is a characteristic critical temperature where the two gaps are the same and near the standard BCS gap parameter of 3.53. We can see that going from the case where the band dispersion is low, i.e. we are close to the regime for a single isolated slab of Blatt to the regime where the dispersion is as large as twice the energy cut-off of the interaction, there are minor variations. This result shows that the shape resonance due to quantum confinement is also a robust feature for appreciable electron hopping between the quantum wells.

6. Conclusions

The present work provides an interpretation of the properties of quantum size effects in superconducting multilayers and indicates a possible roadmap for the discovery of novel HTS like graphene bilayers and graphane superlattices that should share similarities with the known multigap HTS families where the shape resonance is driven by the interband pairing mechanisms.

Here we have investigated the effect of electron hopping between quantum wells that can be changed by changing the thickness of spacer layers, like in 1111 pnictides where the rare earth ionic radius in the spacer layer can be changed, or by changing the type of material forming the spacers, like in going from 1111 to 122 pnictides. To take into account this effect on the shape resonance, we changed the dispersion ξ while keeping it of the order of the pairing interaction energy cut-off ω_0. We have fixed in our calculation the intraband Cooper pairing to be much weaker than the exchange-like interband repulsive interaction. This is clearly the case of iron pnictides that exhibit critical temperatures of the order of 50 K mostly driven by interband pairing. Namely, we have examined the case of the intraband and interband coupling parameter ratio $c_{2,2}/c_{1,1} = 0.45$ with variable interband repulsive interactions and variable single electron dispersion in the transverse direction.

The ratios $2\Delta_1/T_c$ and $-2\Delta_2/T_c$ predicted for high-T_c iron-based layered compounds and cuprates as functions of T_c show that for the highest T_c samples the gaps become equivalent while they are quite different in the low T_c samples, which appears to be the scenario for cuprates and for pnictides. The antiresonance typical of shape resonance occurs where the Lifshitz energy parameter is zero (i.e. the appearance of a new Fermi surface spot) for weak interband exchange pairing and shifts to -1 for a very strong interband exchange pairing. The relevant result is that the maximum of the critical temperature appears near the Lifshitz transition of the type opening a neck in corrugated cylindrical surface therefore it moves with the variation of the electronic hopping between the layers, i.e. the energy dispersion in the normal direction with respect to the superconducting layers.

Acknowledgments

We thank Andrea Perali, Ilya Eremin, and Andrei Shanenko for useful discussions.

References

[1] Bianconi A, De Santis M, Di Cicco A, Flank A M, Fontaine A, Lagarde P, Yoshida H K, Kotani A and Marcelli A 1988 *Phys. Rev.* B **38** 7196
[2] Kristoffel N, Konsin P and Ord T 1994 *Riv. Nuovo Cimento* **17** 1
[3] Kristoffel N, Rubin P and Ord T 2008 *J. Phys.: Conf. Ser.* **108** 012034
[4] Muller K A and Bussmann-Holder A 2005 *Superconductivity in Complex Systems* (Berlin: Springer)
[5] Lifshitz I M 1960 *J. Exp. Theor. Phys. (USSR)* **38** 1569–76 (in Russian)
Lifshitz I M 1960 *Sov. Phys.—JEPT* **11** 1130 (Engl. Transl.)
[6] Varlamov A A, Egorov V S and Pantsulaya A V 1989 *Adv. Phys.* **38** 469
[7] Markiewicz R 1988 *Physica* C **153–155** 1181–2
[8] Bianconi A 1994 *Solid State Commun.* **89** 933
[9] Bianconi A 1998 High T_c superconductors made by metal heterostructures at the atomic limit *European Patent* 0733271
[10] Bianconi A 2001 Process of increasing the critical temperature T_c of a bulk superconductor by making metal heterostructures at the atomic limit *US Patent Specification* 6,265,019 B1 URL http://patft.uspto.gov/
[11] Bianconi A 2005 *J. Supercond.* **18** 25
[12] Bianconi A 2006 *Symmetry and Heterogeneity in high temperature superconductors* (*Nato Science Series II Mathematics, Physics and Chemistry* vol 214) (Dordrecht: Springer)
[13] Bianconi A 2006 *Iran. J. Phys. Res.* **6** 139–47
[14] Khasanov R, Strassler S, Di Castro D, Masui T, Miyasaka S, Tajima S, Holder A B and Keller H 2007 *Phys. Rev. Lett.* **99** 237601
[15] Hufner S, Hossain M A, Damascelli A and Sawatzky G A 2008 *Rep. Prog. Phys.* **71** 062501
[16] Boyer M C, Wise W D, Chatterjee K, Yi M, Kondo T, Takeuchi T, Ikuta H and Hudson E W 2007 *Nat. Phys.* **3** 802
[17] Feng D L *et al* 2002 *Phys. Rev. Lett.* **88** 107001
[18] Doiron-Leyrand N *et al* 2007 *Nature* **447** 565
[19] Yelland E A, Singleton J, Mielke C H, Narrison N, Balakirev F F, Dabrowski B and Cooper J R 2008 *Phys. Rev. Lett.* **100** 047003
[20] Kugel K I, Rakhmanov A L, Sboychakov A O, Poccia N and Bianconi A 2008 *Phys. Rev.* B **78** 165124
[21] Innocenti D, Ricci A, Poccia N, Campi G, Fratini M and Bianconi A 2009 *J. Supercond. Novel Magn.* **22** 529
[22] Doiron-Leyraud N *et al* 2007 *Nature* **447** 565–8
[23] Singleton J *et al* 2010 *Phys. Rev. Lett.* **104** 086403
[24] Sebastian S E *et al* 2010 *Phys. Rev.* B **81** 214524
[25] Norman M 2010 *Physics* **3** 86
[26] Ovchinnikov S G, Korshunov M M and Shneyder E I 2009 *J. Exp. Theor. Phys.* **109** 775–85
[27] Norman M R, Lin J and Millis A J 2010 *Phys. Rev.* B **81** 180513
[28] Tsuda S, Yokoya T, Kiss T, Takano Y, Togano K, Kito H, Ihara H and Shin S 2001 *Phys. Rev. Lett.* **87** 177006

[29] Bussmann-Holder A and Bianconi A 2003 *Phys. Rev.* B **67** 132509
[30] Tsuda S *et al* 2005 *Phys. Rev.* B **72** 064527
[31] Cooley L D, Zambano A J, Moodenbaugh A R, Klie R F, Zheng J-C and Zhu Y 2005 *Phys. Rev. Lett.* **95** 267002
[32] Innocenti D, Poccia N, Ricci A, Valletta A, Caprara S, Perali A and Bianconi A 2010 *Phys. Rev.* B **82** 184528
[33] Bianconi A, Di Castro D, Agrestini S, Campi G, Saini N L, Saccone A, Negri S D and Giovannini M 2001 *J. Phys.: Condens. Matter* **13** 7383
[34] Chen C T, Tsuei C C, Ketchen M B, Ren Z A and Zhao Z X 2010 *Nat. Phys.* **6** 260
[35] Kuroki K, Onari S, Arita R, Usui H, Tanaka Y, Kontani H and Aoki H 2008 *Phys. Rev. Lett.* **101** 087004
[36] Caivano R *et al* 2009 *Supercond. Sci. Technol.* **22** 014004
[37] Bianconi A 2006 *Phys. Status Solidi* a **203** 2950
[38] Lozovik Yu E and Sokolik A A 2009 *Phys. Lett.* A **374** 326
[39] Kristoffel N and Rago K 2010 arXiv:1003.5083
[40] Annett J, Kusmartsev F and Bianconi A 2009 *Supercond. Sci. Technol.* **22** 010301
[41] Bianconi A 2006 *J. Phys. Chem. Solids* **67** 567
[42] Bianconi A, Saini N L, Agrestini S, Di Castro D and Bianconi G 2000 *Int. J. Mod. Phys.* B **14** 3342
[43] Bianconi A, Agrestini S, Bianconi G, Di Castro D and Saini N L 2001 *J. Alloys Compounds* **317/318** 537
[44] Bianconi A, Poccia N and Ricci A 2009 *J. Supercond. Novel Magn.* **22** 527
[45] Ricci A *et al* 2010 *Phys. Rev.* B **82** 144507
[46] Blatt J M and Thompson C J 1963 *Phys. Rev. Lett.* **10** 332
[47] Shanenko A A and Croitoru M D 2006 *Phys. Rev.* B **73** 012510
[48] Bianconi A, Saini N L, Rossetti T, Lanzara A, Perali A, Missori M, Oyanagi H, Yamaguchi H, Nishihara Y and Ha D H 1996 *Phys. Rev.* B **54** 12018
[49] Perali A, Bianconi A, Lanzara A and Saini N L 1996 *Solid State Commun.* **100** 181
[50] Bianconi A, Valletta A, Perali A and Saini N L 1998 *Physica* C **296** 269
[51] Bianconi A, Agrestini S and Bussmann-Holder A 2004 *J. Supercond.* **17** 205
[52] Angilella G G N, Bianconi A and Pucci R 2005 *J. Supercond. Novel Magn.* **18** 19
[53] Filippi M, Bianconi A and Bussmann-Holder A 2005 *J. Physique* IV **131** 49
[54] Rodriguez Nunez J, Schmidt A, Bianconi A and Perali A 2008 *Physica* C **468** 2299
[55] Esposito S, Recami E, van der Merwe A and Battiston R 2009 *Ettore Majorana: Unpublished Research Notes on Theoretical Physic* (*Fundamental Theories of Physics* vol 159) ed S Esposito, E Recami, A van der Merwe and R Battiston (Berlin: Springer) ISBN 1402091133 (doi:10.1007/978-1-4020-9114-8)
[56] Di Grezia E and Esposito S 2008 *Found. Phys.* **38** 228
[57] Vittorini-Orgeas A and Bianconi A 2009 *J. Supercond. Novel Magn.* **22** 215
[58] Blatt J M and Weisskopf V F 1952 *Theoretical Nuclear Physics* (New York: Wiley) p 401
[59] Feshbach H, Porter C E and Weisskopf V F 1954 *Phys. Rev.* **96** 448
[60] de Shalit A and Feshbach H 1974 *Theoretical Nuclear Physics: Nuclear Structure* vol 1 (New York: Wiley) p 87
[61] Hahn Y, O'Malley T F and Spruch L 1962 *Phys. Rev.* **128** 932
[62] O'Malley T F 1966 *Phys. Rev.* **150** 14
[63] Bardsley J N and Mandl F 1968 *Rep. Prog. Phys.* **31** 471
[64] Chin C, Grimm R, Julienne P and Tiesinga E 2010 *Rev. Mod. Phys.* **82** 1225
[65] Tiesinga E, Verhaar B J and Stoof H T C 1993 *Phys. Rev.* A **47** 4114
[66] Inouye S, Andrews M R, Stenger J, Miesner H J, Stamper-Kurn D M and Ketterle W 1998 *Nature* **392** 151
[67] Duine R and Stoof H T C 2004 *Phys. Rep.* **396** 115
[68] Fano U 1935 *Nuovo Cimento* **128** 156
[69] Fano U 1961 *Phys. Rev.* **124** 1866
[70] Feshbach H 1958 *Ann. Phys., NY* **5** 357
[71] Agrestini S, Saini N L, Bianconi G and Bianconi A 2003 *J. Phys. A: Math. Gen.* **36** 9133
[72] Fratini M, Poccia N and Bianconi A 2008 *J. Phys.: Conf. Ser.* **108** 012036
[73] Poccia N and Fratini M 2009 *J. Supercond. Novel Magn.* **22** 299
[74] Bianconi A, Di Castro D, Saini N L and Bianconi G 2002 *Phase Transitions and Self-Organization in Electronic and Molecular Networks Fundamental Materials Research* ed M F Thorpe and J C Phillips (Boston, MA: Kluwer) chapter 24, pp 375–88 (Academic) (doi:org/10.1007/0-306-47113-2-24)
[75] Bianconi A 2000 *Int. J. Mod. Phys.* B **14** 3289
[76] Saini N L and Bianconi A 2000 *Int. J. Mod. Phys.* B **14** 3649
[77] Hirsch J E and Scalapino D J 1986 *Phys. Rev. Lett.* **56** 2732
[78] Labbe J and Bok J 1987 *Europhys. Lett.* **3** 1225
[79] Newns D M, Tsuei C C and Pattnaik P C 1995 *Phys. Rev.* B **52** 13611
[80] Markiewicz R 1997 *J. Phys. Chem. Solids* **58** 1179
[81] Cappelluti E and Pietronero L 1996 *Phys. Rev.* B **53** 932
[82] Halboth C J and Metzner W 2000 *Phys. Rev. Lett.* **85** 5162
[83] Yamase H and Metzner W 2007 *Phys. Rev.* B **75** 155117
[84] Ho A F and Schofield A J 2008 *Europhys. Lett.* **84** 27007
[85] Dagotto E 1994 *Rev. Mod. Phys.* **66** 763
[86] Imada M, Fujimori A and Tokura Y 1998 *Rev. Mod. Phys.* **70** 1039
[87] Ovchinnikov S G 1997 *Phys.—Usp.* **40** 993
[88] Maksimov E G 2000 *Phys.—Usp.* **43** 965
[89] Bianconi A, Saini N L, Lanzara A, Missori M, Rossetti T, Oyanagi H, Yamaguchi H, Oka K and Ito T 1996 *Phys. Rev. Lett.* **76** 3412
[90] Saini N L *et al* 1997 *Phys. Rev. Lett.* **79** 3467–70
[91] Lebegue S, Yin Z P and Pickett W E 2009 *New J. Phys.* **11** 025004
[92] Mazov L S 2009 arXiv:0911.4089
[93] Shishido H *et al* 2010 *Phys. Rev. Lett.* **104** 057008
[94] Cao G, Jiang S, Wang C, Li Y, Ren Z, Tao Q, Dai J and Xu Z-A 2009 *Physica* C **470** S458
[95] Wang C, Jiang S, Tao Q, Ren Z, Li Y, Li L, Feng C, Dai J, Cao G and Xu Z-A 2009 *Europhys. Lett.* **86** 47002
[96] Dai J, Si Q, Zhu J-X and Abrahams E 2009 *Proc. Natl Acad. Sci.* **106** 4118
[97] Terashima K *et al* 2009 *Proc. Natl Acad. Sci.* **106** 7330
[98] Perali A, Pieri P and Strinati G C 2004 *Phys. Rev. Lett.* **93** 100404
[99] Leggett A J 1980 *Modern Trends in the Theory of Condensed Matter* (*Lecture Notes in Physics* vol 115) ed A Pekalski and R Przystawa (Berlin: Springer) p 13
[100] Entel P and Rainer D 1976 *J. Low Temp. Phys.* **23** 511
[101] Ma F, Lu Z-Y and Xiang T 2010 *Front. Phys. China* **5** 150
[102] Nekrasov I A, Pchelkina Z V and Sadovskii M V 2008 *JETP Lett.* **88** 144–9
[103] Ding H *et al* 2008 *Europhys. Lett.* **83** 47001
[104] Zabolotnyy V B *et al* 2009 *Physica* C **469** 448–51
[105] Liu C *et al* 2008 *Phys. Rev. Lett.* **101** 177005
[106] Wray L *et al* 2008 *Phys. Rev.* B **78** 184508
[107] Liu C *et al* 2009 *Phys. Rev. Lett.* **102** 167004
[108] Kondo T *et al* 2008 *Phys. Rev. Lett.* **101** 147003
[109] Yang L X *et al* 2010 *Phys. Rev.* B **82** 104519
[110] He C *et al* 2010 *J. Phys. Chem. Solids* doi:10.1016/j.jpcs.2010.10.078
[111] Thirupathaiah S *et al* 2010 *Phys. Rev.* B **81** 104512
[112] Vilmercati P *et al* 2009 *Phys. Rev.* B **79** 220503